Intrinsic Double-Stranded-RNA Processing Activity of *Escherichia coli* Ribonuclease III Lacking the dsRNA-Binding Domain†

Weimei Sun, Eunjoo Jun, and Allen W. Nicholson*

Department of Biological Sciences, Wayne State University, 5047 Gullen Mall, Detroit, Michigan 48202

Received July 27, 2001; Revised Manuscript Received September 24, 2001

ABSTRACT: The ribonuclease III superfamily represents a structurally related group of double-strand (ds) specific endoribonucleases which play key roles in diverse prokaryotic and eukaryotic RNA maturation and degradation pathways. A dsRNA-binding domain (dsRBD) is a conserved feature of the superfamily and is important for substrate recognition. RNase III family members also exhibit a "catalytic" domain, in part defined by a set of highly conserved amino acids, of which at least one (a glutamic acid) is important for cleavage but not for substrate binding. However, it is not known whether the catalytic domain requires the dsRBD for activity. This report shows that a truncated form of *Escherichia coli* RNase III lacking the dsRBD (RNase III[ΔdsRBD]) can accurately cleave small processing substrates in vitro. Optimal activity of RNase III[ΔdsRBD] is observed at low salt concentrations (<60 mM Na^+), either in the presence of Mg^{2+} (>25 mM) or Mn^{2+} (∼5 mM). At 60 mM Na^+ and 5 mM Mn^{2+} the catalytic efficiency of RNase III[ΔdsRBD] is similar to that of RNase III at physiological salt concentrations and Mg^{2+}. In the presence of Mg^{2+} RNase III[ΔdsRBD] is less efficient than the wild-type enzyme, due to a higher K_m. Similar to RNase III, RNase III[ΔdsRBD] is inhibited by high concentrations of Mn^{2+}, which is due to metal ion occupancy of an inhibitory site on the enzyme. RNase III[ΔdsRBD] retains strict specificity for dsRNA, as indicated by its inability to cleave $(rA)_{25}$, $(rU)_{25}$, or $(rC)_{25}$. Moreover, dsDNA, ssDNA, or an RNA−DNA hybrid are not cleaved. Low (micromolar) concentrations of ethidium bromide block RNase III-[ΔdsRBD] cleavage of substrate, which is similar to the inhibition seen with RNase III and is indicative of an intercalative mode of inhibition. Finally, RNase III[ΔdsRBD] is sensitive to specific Watson−Crick base-pair substitutions which also inhibit RNase III. These findings support an RNase III mechanism of action in which the catalytic domain (i) can function independently of the dsRBD, (ii) is dsRNA-specific, and (iii) participates in cleavage site selection.

Bacterial RNA processing and decay pathways involve the coordinated action of a diverse set of cellular ribonucleases. Maturation reactions provide fully functional RNAs, while degradation pathways can regulate gene expression by controlling steady-state mRNA levels, as well as provide mononucleotides for new RNA synthesis (for reviews, see refs *1*−*4*). The endo- and exoribonucleases that establish these pathways recognize specific features in their substrates. Double-stranded (ds) structures provide key targets for cleavage and are recognized by members of the ribonuclease III superfamily of endoribonucleases. The most studied member is *Escherichia coli* ribonuclease III, which was first detected as an activity in cell-free extracts that could degrade dsRNA to acid solubility (*5*). A cellular role for RNase III was subsequently determined to be the cleavage of the primary transcripts of the rRNA operons, providing the immediate precursors to the mature species. RNase III also cleaves many other structural and messenger RNAs, including plasmid- and bacteriophage-encoded transcripts. RNase III cleavage of mRNA can enhance translation or initiate turnover with concomitant down-regulation of gene expression (for reviews, see refs *2*, *6*, and *7*).

E. coli RNase III is a phosphodiesterase and requires a divalent metal ion (preferably Mg^{2+}) for activity. Exhaustive cleavage of long dsRNAs provides duplex products ranging in size from ∼11 to 15 bp and which exhibit two nucleotide 3′ overhangs with 5′-phosphate, 3′-hydroxyl termini. Cellular substrates undergo site-specific cleavage, with the cleavage sites determined by Watson−Crick (W−C) base-pair sequences, internal loops, bulges, and base mismatches (*2*, *6*−*10*). The processing of cellular substrates can be accurately reconstructed in vitro using purified enzyme and small transcripts containing the minimal required set of reactivity epitopes (*8*−*12*). The polypeptide elements involved in processing specificity are not known. Thus, while bacterial RNase III orthologues exhibit similar sequences and sizes, the substrate specificities are nonetheless distinct (e.g., see ref *12*). Physiologically relevant salt concentrations (200−300 mM M^+) and Mg^{2+} as the divalent metal ion promote cleavage of canonical (primary) sites (*9*−*11*), while lower salt concentrations and/or replacing Mg^{2+} by Mn^{2+} promotes cleavage of additional ("secondary") sites, which

† This work was supported by NIH Grant GM56457.

* Corresponding author. E-mail: anichol@biology.biosci.wayne.edu. Tel: (313)-577-2862.

[1] Abbreviations: AD, antideterminant; db, distal box; dsRBD, double-stranded RNA-binding domain; dsRNA, double-stranded RNA; DTT, dithiothreitol; EB, ethidium bromide; IPTG, isopropylthio-β-D-galactopyranoside; pb, proximal box; RNase, ribonuclease; TBE, Tris−borate−EDTA; W−C, Watson−Crick.

10.1021/bi011570u CCC: $20.00
Published on Web 11/10/2001

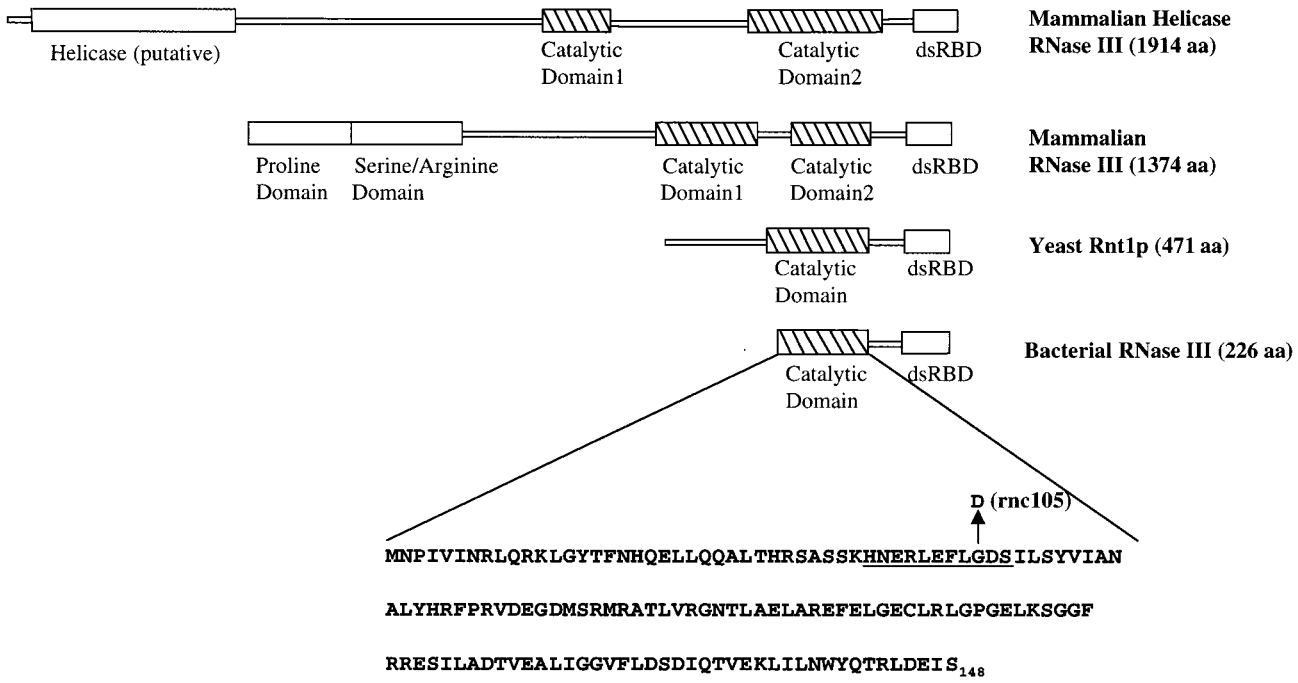

FIGURE 1: Domain structures of type members of the RNase III superfamily. Shown are the domain structures of two mammalian orthologues, the yeast orthologue Rnt1p, and bacterial orthologues. Also shown is the primary sequence of the catalytic domain of *E. coli* RNase III. The portion of the *rnc* gene encoding this sequence was cloned into pET-15b and the purified protein used in this study (see text). The underlined residues indicate the highly conserved signature sequence of RNase III family members (*20*−*22*). The *rnc105* mutation (*16*) is shown.

are not normally recognized in vivo (*13*, *14*). While the molecular basis for secondary site recognition remains obscure, in at least one instance the cleavage of a secondary site can control expression of a bacteriophage gene (*15*).

E. coli RNase III is active as a homodimer, with a subunit size of 25.6 kDa (226 amino acids) (*13*, *16*). The C-terminal portion of the RNase III polypeptide contains a dsRNA-binding domain (dsRBD) (*17*), which is a conserved feature of RNase III family members (Figure 1) and which is present in many other dsRNA-binding proteins with diverse functions (*18*, *19*). The dsRBD is a key participant in the mechanism of RNase III action, as mutations in this domain which reduce dsRNA-binding affinity in vitro exert a proportional inhibition of cleavage of substrate in vitro and in vivo (A. K. Amarasinghe, S. Su, W.S., R. W. Simons, and A.W.N., in preparation). The N-terminal two-thirds of the *E. coli* RNase III polypeptide contains a number of conserved residues, including an ~10 amino acid "signature sequence" which is characteristic of RNase III family members (Figure 1) (*20*−*22*). Evidence that the active site is in this domain is in part based on the observation that mutation of the near-invariant Glutamic acid 117 in *E. coli* RNase III blocks the cleavage step without inhibiting substrate binding (*23*−*25*). Several higher eukaryotic RNase III family members exhibit a duplication of catalytic domain sequences and also contain N-terminal extensions with potential additional activities (Figure 1). In the *S. cerevisiae* homologue Rnt1p, the N-terminal extension is important for dimer stability (*26*). RNase III homologues involved in RNA interference (RNAi) contain a putative DExH/DEAH helicase domain, in addition to a tandem duplicated RNase III catalytic domain, and at least one copy of the dsRBD (*27*, *28*) (Figure 1).

The domain structure of bacterial RNase III orthologues suggests a mechanism of action in which the initial step in processing involves substrate recognition by one or both of the dsRBDs, followed by engagement of the catalytic domain and phosphodiester hydrolysis. The two steps are not inextricably linked, as it has been shown that substrate binding and cleavage can be uncoupled by site-specific intercalation of ethidium bromide into substrate (*29*). However, it is not known whether the catalytic domain contains the necessary and sufficient features for catalysis and, if so, whether or to what extent the catalytic domain confers dsRNA specificity and participates in cleavage site selection. This report describes the intrinsic catalytic activity of a truncated version of *E. coli* RNase III lacking the dsRBD. The implications of these findings on the mechanism of action of RNase III are discussed.

MATERIALS AND METHODS

Materials. Water was deionized and distilled. Chemicals were reagent grade or molecular biology grade and were generally purchased from Sigma (St. Louis, MO) or Fisher Scientific (Chicago, IL). Ethidium bromide was purchased from Sigma and used without further purification. The oligoribonucleotides $(rA)_{25}$, $(rC)_{25}$, and $(rU)_{25}$ were synthesized by Dharmacon Research, Inc. (Lafayette, CO), and were deprotected and purified by gel electrophoresis according to the supplied instructions. Oligodeoxyribonucleotides were synthesized by Invitrogen (Bethesda, MD) or prepared in-house using a Beckman Oligo 1000 synthesizer and were deprotected and purified by gel electrophoresis as described (*30*). The radiolabeled ribonucleoside 5′-triphosphates [α-^{32}P]-CTP (3000 Ci/mmol) and [γ-^{32}P]ATP (3000 Ci/mmol) were purchased from Perkin-Elmer (Boston, MA). Restriction enzymes, T4 DNA ligase, T4 polynucleotide kinase, and Vent DNA polymerase were purchased from New England Biolabs (Beverley, MA). *E. coli* RNase H1 was purchased from Epicentre Technologies (Madison, WI). Calf intestine alkaline phosphatase was obtained from Roche Molecular

Diagnostics (Indianapolis, IN), and T7 RNA polymerase was purified in-house as described (*31*).

Protein Purification. Hexahistidine[$(His)_6$]-tagged RNase III was purified as described (*30*). Construction of a pET-15b recombinant plasmid encoding the truncated form of RNase III (RNase III[ΔdsRBD]) and purification of $(His)_6$-RNase III[ΔdsRBD] are described elsewhere (A. K. Amarasinghe, S. Su, W.S., R. W. Simons, and A. W. N., in preparation). Briefly, the truncated form of RNase III encoding the N-terminal 148 amino acids was overproduced as an N-terminal $(His)_6$-tagged protein. Serine 148 was chosen as the C-terminal residue of RNase III[ΔdsRBD] (see Figure 1) as it is immediately upstream of the N-terminus of the dsRBD. $(His)_6$RNase III[ΔdsRBD] was overproduced by IPTG (1 mM) treatment of the RNase III$^-$ *E. coli* strain BL21(DE3)*rnc105recA* containing the recombinant pET-15b plasmid (*30*). Use of this expression host served to avoid contamination with chromosomally encoded RNase III. The overproduced $(His)_6$RNase III[ΔdsRBD] was present in both the soluble and insoluble portions of sonicated cell extracts. The protein was purified from the soluble portion by Ni^{2+} affinity chromatography, with an estimated purity of >90%, as assessed by SDS−PAGE and Coomassie staining. The yield of soluble $(His)_6$RNase III[ΔdsRBD] was ∼0.6 mg/L of cell culture. $(His)_6$RNase III[ΔdsRBD] retains normal dimeric behavior, as revealed by gel filtration and chemical cross-linking (A. K. Amarasinghe, S. Su, W.S., R. W. Simons, and A. W. N., in preparation). Since the $(His)_6$-tag has no significant effect on the activity of RNase III (*30*), it was assumed that the same holds true with RNase III-[ΔdsRBD]. For the purposes of this report, $(His)_6$RNase III-[ΔdsRBD] will be referred to as RNase III[ΔdsRBD].

Substrate Synthesis. The RNase III processing substrates R1.1 RNA (*9*) and R1. 1[WC] RNA (*8*) (see Figures 2A and 7A, respectively) were enzymatically synthesized as described (*30*). Internally ^{32}P-labeled substrates were prepared by including [α-^{32}P]CTP (final specific activity ∼100 Ci/mol) in the transcription reaction. To prepare 5′-^{32}P-labeled R1.1 RNA, gel-purified nonradioactive transcript was dephosphorylated with Calf intestine alkaline phosphatase and then treated with [γ-^{32}P]ATP (3000 Ci/mmol) and T4 polynucleotide kinase. Both types of radiolabeled RNAs were purified by electrophoresis in polyacrylamide/7M urea gels as described (*30*). The RNAs were stored in TE buffer (pH 7.5) at −20 °C.

Substrate Cleavage Assay. Substrate cleavage assays were performed as described (*24*, *30*) using internally ^{32}P-labeled R1.1 RNA. The reaction times, enzyme concentrations (reported as dimer species), and buffer components are provided in the appropriate figure or table legend. Reactions were analyzed by electrophoresis in 15% or 20% polyacrylamide gels containing 7 M urea and TBE (or 0.5 × TBE) buffer and were visualized and quantitated by phosphorimaging (Molecular Dynamics Storm 860 System) as described (*24*, *30*). Determination of steady-state kinetic parameters was carried out as described in ref *24* using Kaleidagraph software (Reading, PA).

RESULTS

The N-terminal two-thirds of the *E. coli* RNase III polypeptide contains a number of conserved residues, of which one (Glu117) is essential for phosphodiester hydrolysis but not for substrate binding (*23*, *24*). It is shown elsewhere that a truncated form of RNase III specifically lacking the dsRBD (RNase III[ΔdsRBD]) retains normal dimeric behavior but does not exhibit detectable activity in vivo (A. K. Amarasinghe, S. Su, W.S., R. W. Simons, and A. W. N., in preparation). Since RNase III can cleave substrate in vitro in a variety of nonphysiological conditions (*13*, *14*), we assessed the activity of purified RNase III[ΔdsRBD] in vitro under such conditions. The substrate is R1.1 RNA (Figure 2A), a 60 nt transcript corresponding to the bacteriophage T7 R1.1 RNase III processing signal (*32*). R1.1 RNA undergoes enzymatic cleavage at a single phosphodiester within the internal loop, providing products of 47 and 13 nt in length. At low salt concentrations cleavage occurs also at a secondary site on the opposite side of the internal loop (Figure 2A) (*11*).

A cleavage assay using internally ^{32}P-labeled R1.1 RNA is shown in Figure 2B. In physiological salt conditions (300 mM NaCl; Mg^{2+}), where RNase III carries out the expected reaction (Figure 2B, lane 2), RNase III[ΔdsRBD] fails to cleave substrate (Figure 2B, lane 3). However, under conditions of low salt (60 mM Na^+) and an alternative divalent metal ion (Mn^{2+}, 5 mM), RNase III[ΔdsRBD] cleaves R1.1 RNA, yielding the same set of products as RNase III (Figure 2B, lane 5). It is important in this regard to note that a 15% polyacrylamide−7 M urea gel can allow detection of even a single nucleotide shift in cleavage site for these small substrates (*8*). There is also some cleavage of the secondary site, as evidenced by the appearance of the "1° + 2°" product (Figure 2B, lane 5). Under these conditions RNase III exhibits low activity, in part because 5 mM Mn^{2+} confers inhibition (*24*) (see also below). We also examined the activity of RNase III[ΔdsRBD] containing the *rnc105* mutation (Gly44Asp) (Figure 1) which inactivates RNase III (*16*, *33*). No cleavage of substrate was observed with purified RNase III[ΔdsRBD](Gly44Asp) under a variety of conditions (data not shown). Thus, a mutation which inactivates RNase III also has a similar effect on RNase III-[ΔdsRBD].

Characterization of Factors That Support Catalytic Activity of RNase III[ΔdsRBD]. The salt concentration and the divalent metal ion concentration were varied to identify conditions which promote optimal activity of RNase III-[ΔdsRBD]. To maximize detection of any change in cleavage activity in response to a change in variable, the chosen reaction times and enzyme concentrations allowed only a limited amount of cleavage. Lowering the salt concentration yields a progressively greater amount of cleavage, either in the presence of Mn^{2+} (1 mM) (Figure 3, lanes 1−7) or Mg^{2+} (10 mM) (Figure 3, lanes 8−14). The enhancement of substrate cleavage by a reduction in salt concentration indicates that ionic interactions play an important role in promoting RNase III[ΔdsRBD] activity. The dependence of substrate cleavage on the divalent metal ion type and concentration was determined at a fixed salt concentration (60 mM NaCl). Figure 4 shows that the optimal Mg^{2+} concentration is reached by ∼20 mM, while the optimal concentration of Mn^{2+} is ∼5 mM. A sharp inhibition occurs at higher Mn^{2+} concentrations but not at elevated Mg^{2+} concentrations (Figure 4). The overall dependence of RNase III[ΔdsRBD] activity on the Mn^{2+} concentration is similar

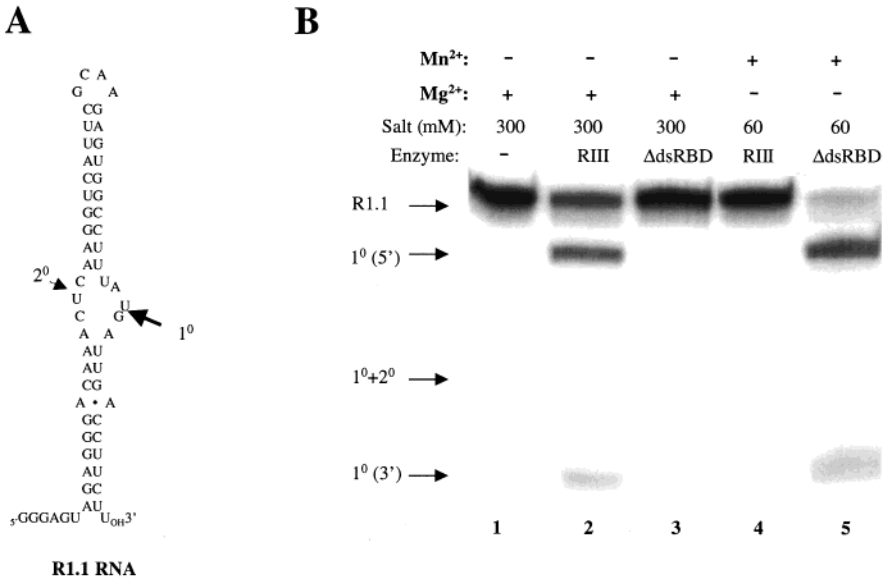

FIGURE 2: Substrate cleavage in vitro by RNase III[ΔdsRBD]. (A) Sequence and secondary structure of R1.1 RNA. The primary and secondary cleavage sites are indicated. (B) Cleavage assays using internally ^{32}P-labeled R1.1 RNA. Assays were performed at 37 °C for 2 min, using the specified enzyme concentrations (given below), as described in Materials and Methods. The salt (NaCl) concentrations are indicated above each lane, as are the divalent metal ion species used (Mg^{2+}, 25 mM; Mn^{2+}, 5 mM). The reaction products were electrophoresed in a 20% polyacrylamide−7 M urea gel and were visualized by phosphorimaging. Lane 1: R1.1 RNA incubated in physiological salt (300 mM NaCl) and Mg^{2+} without enzyme. Lane 2: reaction in physiological salt in the presence of RNase III (24 nM). Lane 3: reaction in physiological salt in the presence of RNase III[ΔdsRBD] (100 nM). Lane 4: Reaction in low salt/Mn^{2+} with RNase III (24 nM). Lane 5: reaction in low salt/Mn^{2+} with RNase III[ΔdsRBD] (100 nM).

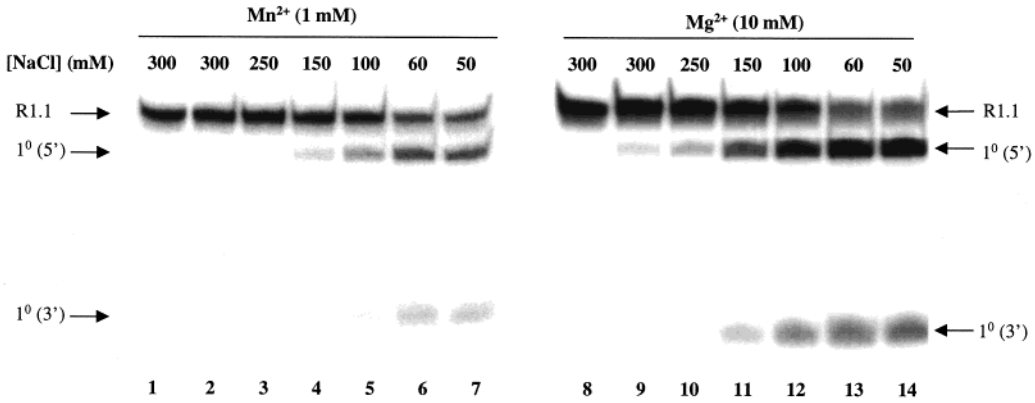

FIGURE 3: Effect of salt concentration on RNase III[ΔdsRBD] cleavage of substrate. Cleavage reactions were performed as described in Materials and Methods, using internally ^{32}P-labeled R1.1 RNA and RNase III[ΔdsRBD] (200 nM). Reactions were analyzed by electrophoresis in a 20% polyacrylamide−urea gel and visualized by phosphorimaging. The positions of the substrate and the two cleavage products are indicated on the right-hand side. Lanes 1−7: RNase III[ΔdsRBD] cleavage of substrate in the presence of 1 mM Mn^{2+} (reaction time, 25 min.). Lanes 8−14: RNase III[ΔdsRBD] (reaction time, 30 min.).

to that seen with RNase III, except that the optimal concentration is ∼5 mM instead of 1 mM. On the basis of the results of a previous study (*24*), the inhibition reflects Mn^{2+} occupancy of an inhibitory site on the enzyme (see also Discussion).

The catalytic efficiencies of RNase III[ΔdsRBD] and RNase III were compared under the respective optimal reaction conditions. Figure 5 shows the substrate concentration dependence of initial rate of R1.1 RNA cleavage by RNase III[ΔdsRBD] either in the presence of 25 mM Mg^{2+} or 5 mM Mn^{2+}. In each case, saturation of the initial velocity occurs as a function of substrate concentration. The fitted curves show that Mn^{2+} is more effective than Mg^{2+} in promoting cleavage at lower substrate concentrations. The steady-state kinetic parameters were determined by least-squares analysis and are provided in Table 1. The data show that in the presence of 5 mM Mn^{2+}, RNase III[ΔdsRBD] possesses a catalytic efficiency (k_{cat}/K_m) essentially the same as that of RNase III under its optimal conditions. Although Mg^{2+} can also support RNase III[ΔdsRBD] activity, K_m is approximately 10-fold greater, while k_{cat} is essentially unchanged. The difference in K_m values suggests that deletion of the dsRBD weakens substrate affinity, which is only partly rescued by low salt and high Mg^{2+} but which is essentially fully restored in the presence of low salt and 5 mM Mn^{2+} (see Discussion).

RNase III[ΔdsRBD] Retains Double-Stranded-RNA Specificity. RNase III does not recognize ssRNA, DNA, or RNA−DNA hybrids (*6, 34*). The stringent specificity for dsRNA may be conferred by the dsRBD, which only recognizes dsRNA (*18, 19*). It is therefore possible that removal of the dsRBD may broaden or otherwise alter the range of reactive substrates. We tested the ability of RNase III[ΔdsRBD] to cleave the synthetic ssRNAs $(rA)_{25}$, $(rC)_{25}$, and $(rU)_{25}$. These

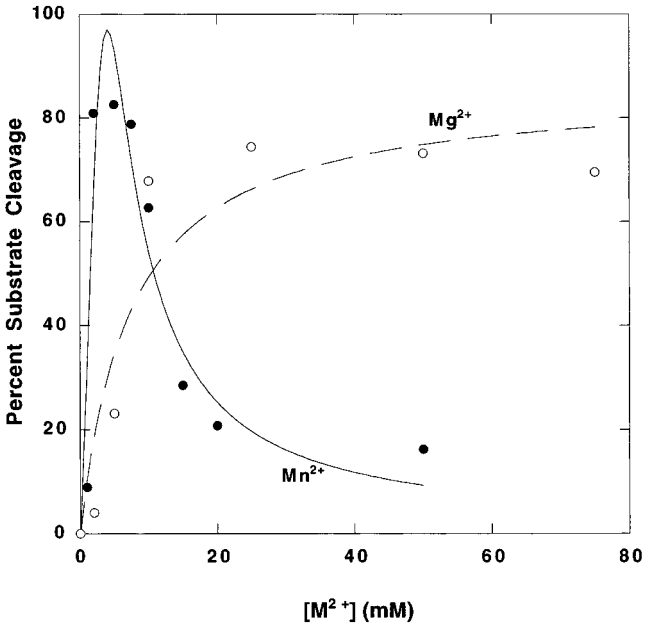

FIGURE 4: Efficiency of substrate cleavage by RNase III[ΔdsRBD] as a function of divalent metal type and concentration. Cleavage reactions were carried out using internally ^{32}P-labeled R1.1 RNA, RNase III[ΔdsRBD] (200 nM), and 60 mM NaCl for 20 min at 37° at the indicated metal ion concentrations. Data were fitted to spline curves, using either a single affinity class of divalent metal binding site (Mg^{2+}), or a single activator site and a single inhibitory site (Mn^{2+}) (see also ref *24*). Open circles: Mg^{2+} dependence of cleavage. Filled circles: Mn^{2+} dependence of cleavage.

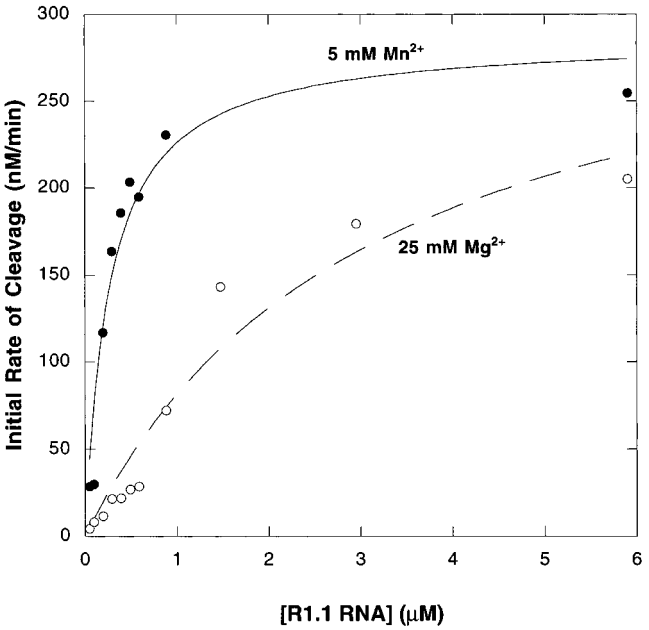

FIGURE 5: Dependence of initial rate of cleavage on substrate concentration and divalent metal ion identity. For the Mg^{2+} experiment (open circles) initial cleavage rates were measured using R1.1 RNA, 100 nM RNase III[ΔdsRBD], and 25 mM Mg^{2+} for 5 min at the indicated substrate concentrations. For the Mn^{2+} experiment (closed circles) initial cleavage rates were measured using R1.1 RNA, 50 nM RNase III[ΔdsRBD], and 5 mM Mn^{2+} for 1 min at the indicated substrate concentrations. Reactions were electrophoresed in a 15% polyacrylamide−7 M urea gel and were quantitated by phosphorimaging. Curve fitting was carried out by assuming Michaelis−Menten kinetics (*11, 24*). The K_m and k_{cat} values are provided in Table 1.

sequences were chosen to avoid possible secondary structure elements, which can occur in "random" sequence ssRNAs (e.g., those generated by transcription of heteropolymeric templates) and which could provide adventitious cleavage sites. Also, the 25 nucleotide length is greater than the minimum length for RNase III substrates, which has been proposed to be two turns of the 11-fold A-helix (*6, 34*). Cleavage assays using the 5′-^{32}P-labeled ssRNAs reveal that none of the species are cleaved by RNase III under a variety of reaction conditions (data not shown). We also tested whether a large excess of each ssRNA could inhibit RNase III[ΔdsRBD] cleavage of ^{32}P-labeled R1.1 RNA. No significant inhibition of cleavage was observed at a ssRNA/substrate molar ratio of 200:1 (data not shown). We next tested whether RNase III[ΔdsRBD] could cleave an RNA−DNA hybrid, prepared by annealing ^{32}P-labeled R1.1 RNA to its ssDNA template. Under conditions where the hybrid is efficiently cleaved by *E. coli* RNase H1, there is no detectable cleavage using a high concentrations (>100 nM) of RNase III[ΔdsRBD] (data not shown). Finally, RNase III[ΔdsRBD] did not cleave the 77 nt ssDNA transcription template for R1.1 RNA, nor could it cleave the pET-15b or pBlueScript plasmids (data not shown). We conclude that RNase III[ΔdsRBD] retains strict specificity for dsRNA.

Table 1: Comparison of Steady-state Catalytic Parameters for RNase III[ΔdsRBD] and RNase III[a]

	RNase III [ΔdsRBD]	RNase III	RNase III [ΔdsRBD]	RNase III
M^{2+} (mM)	25 (Mg^{2+})	5 (Mg^{2+})	5 (Mn^{2+})	1 (Mn^{2+})
k_{cat} (min^{-1})	3.1(±0.6)	3.8	2.9(±0.2)	1.4
K_m (nM)	3000(±1000)	335	271(±66)	110
k_{cat}/K_m ($M^{-1}min^{-1}$)	1.1×10^6	1.1×10^7	1.1×10^7	1.3×10^7

[a] Cleavage assays were performed as described in Materials and Methods using purified RNase III[ΔdsRBD] and internally ^{32}P-labeled R1.1 RNA. Experimental conditions were chosen which allowed only limited (<30%) conversion to product. The data for the RNase III experiments were from ref *24*. Previously determined K_m and k_{cat} values for RNase III (lacking the His_6-tag, and in 10 mM Mg^{2+}) are 330 nM and 1.8 min^{-1}, respectively (*11*). The divalent metal species and concentrations are indicated, and the salt (NaCl) concentration was 60 mM. In the Mg^{2+} experiment, the RNase III[ΔdsRBD] concentration was 100 nM (dimer). In the Mn^{2+} experiment, the RNase III[ΔdsRBD] concentration was 50 nM (dimer). Nonlinear least-squares analysis was carried out, assuming Michaelis−Menten behavior (*11, 24*). The kinetic assays were performed at least two times. The reported values are from a single experiment (standard errors from curve fitting given in the parentheses). The exact experimental conditions (e.g., reaction times and enzyme concentrations) differed in each experiment, and thereby did not allow averaging of the duplicate experiments.

Inhibition of RNase III[ΔdsRBD] by Ethidium Bromide. Ethidium bromide (EB) is a dsRNA intercalating agent which can block RNase III cleavage of substrate without strongly inhibiting the binding step (*29*). EB site-specifically binds to R1.1 RNA to cause apparent competitive inhibitory kinetics but does not affect RNase III binding to substrate (*29*). Given the dsRNA specificity of the truncated enzyme (see above), a prediction is that EB would also inhibit RNase III[ΔdsRBD] cleavage of substrate. To test this, cleavage assays were performed which measured RNase III[ΔdsRBD] cleavage of R1.1 RNA as a function of EB concentration, either in the presence of Mg^{2+} (25 mM) or Mn^{2+} (5 mM). The results are shown in Figure 6, which reveal that in each case EB confers inhibition. In the presence of Mg^{2+}, an EB concentration of ~10 μM provides half-maximal inhibition, while in the presence of Mn^{2+} it is ~40 μM. These inhibitory concentrations are consistent with an intercalative mechanism

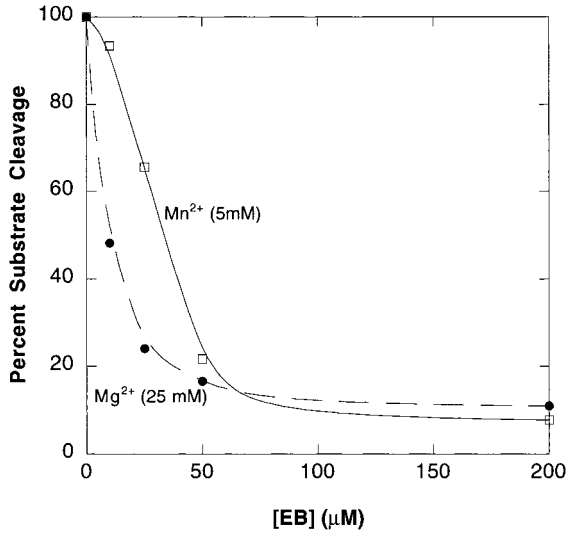

FIGURE 6: Ethidium bromide inhibition of RNase III[ΔdsRBD]. Cleavage reactions used internally ^{32}P-labeled R1.1 RNA and included ethidium bromide (EB) at the indicated concentrations. The extent of substrate cleavage in the absence of EB was normalized to 100%. The two curves show the concentration dependence of EB inhibition of R1.1 RNA cleavage, either in the presence of Mg^{2+} (25 mM) (closed circles) or Mn^{2+} (5 mM) (open squares).

of inhibition (*29*). We conclude that EB inhibition of RNase III[ΔdsRBD] mirrors its ability to inhibit RNase III and reflects a disrupted interaction of RNase III[ΔdsRBD] with the substrate−ethidium complex (see also Discussion).

RNase III[ΔdsRBD] Is Inhibited by Watson−Crick bp Antideterminants. The conserved pattern of substrate cleavage by RNase III[ΔdsRBD] and RNase III indicates that the catalytic domain is a key participant in cleavage site selection. To examine this further we tested whether specific mutations in substrate which inhibit RNase III could also inhibit RNase III[ΔdsRBD]. It has been shown that specific Watson−Crick (W−C) bp substitutions in either of two regions in an RNase III substrate can block cleavage by inhibiting enzyme binding (*8*). These inhibitory W−C bp have been termed "antideterminants"—in analogy to antideterminant (AD) sequence elements in tRNAs which control tRNA−protein transactions (*35*)—which have been proposed to participate in cleavage site selection, as well as protect intracellular dsRNAs with vital functions from unwanted cleavage (*8*). We introduced specific W−C bp substitutions into R1.1[WC] RNA (Figure 7A), which is a variant of R1.1 RNA containing a fully W−C base-paired internal loop. R1.1[WC] RNA is cleaved at two sites to provide three products of 8, 10, and 28 nt in size (*8*). W−C bp substitutions shown elsewhere to inhibit RNase III (*8*) were introduced either into the 3 bp proximal box (pb) or the 2 bp distal box (db) (Figure 7A). The 3 bp substitution in the pb of N84 RNA corresponds to the $tRNA^{Sec}$ AD sequence, which blocks EF−Tu·GTP binding to $tRNA^{Sec}$ (*35*) and which also has been shown to inhibit RNase III cleavage of R1.1[WC] RNA (*8*). We also prepared the closely related variant, N90 RNA, in which the AD sequence was positioned instead between the db and pb. This substitution does not inhibit cleavage by RNase III (*8*). The third variant, N152 RNA, incorporates a 2 bp inhibitory W−C bp substitution in the db (Figure 7A).

Cleavage assays using internally ^{32}P-labeled substrate are shown in Figure 7B−D. The RNase III assays were performed at physiological salt concentrations and 5 mM Mg^{2+}, while the assays with RNase III[ΔdsRBD] were performed in low salt and 25 mM Mg^{2+}. The presence of the $tRNA^{Sec}$ AD sequence in the pb inhibits RNase III[ΔdsRBD] action, in addition to inhibiting RNase III (compare lanes 1−6, Figure 7C, with lanes 1−6, Figure 7B). Quantitative analysis (Table 2) reveals that N84 RNA is cleaved by RNase III[ΔdsRBD] at less than half the rate than R1.1[WC] RNA. In contrast, placing the AD sequence between the pb and db does not cause inhibition of RNase III[ΔdsRBD] action (compare lanes 1−3 and 7−9 in both Figure 7B,C, and see Table 2). These patterns of reactivity reflect that seen with RNase III, although the effects of the pb and db mutations on RNase III are stronger (see Table 2). We believe that the smaller inhibitory effect of the mutations on RNase III[ΔdsRBD] action reflects an effect of low salt concentration, which has been shown to enhance RNase III cleavage of unreactive substrates relative to the parent substrate (W.S., K. Zhang and A.W.N, unpublished). The assays also show that RNase III[ΔdsRBD] cleaves R1.1[WC] RNA at the two canonical sites (compare lanes 1−3 in both Figure 7B,C). However, there is some accumulation of the singly cleaved species (lanes 2 and 3, Figure 7C), which may reflect the weaker binding of RNase III[ΔdsRBD], allowing dissociation of enzyme prior to cleavage of the second phosphodiester.

The incorporation of a W−C bp sequence in the db of R1.1[WC] RNA also inhibits RNase III[ΔdsRBD] (compare lanes 7−9 with lanes 4−6, Figure 7C). Quantitative analysis (Table 2) reveals that N152 RNA is cleaved by RNase III[ΔdsRBD] at one-third the rate, seen using R1.1[WC] RNA as substrate. Similar to the effects of the pb mutation effect, RNase III is more strongly inhibited by the db mutation. The experiment also shows that RNase III[ΔdsRBD] is less efficient than RNase III in cleaving R1.1[WC] RNA (compare lanes 4−6 with 1−3, Figure 7C), as indicated by the accumulation of singly cleaved species (Figure 7D, lanes 1−3). In summary, these experiments establish that inhibitory W−C base-pairs in either the pb or db inhibit the action of RNase III[ΔdsRBD]. The sensitivity of the truncated form of RNase III to antideterminant sequences in the pb and db indicate that the domain participates in cleavage site selection as well as in the catalytic step.

DISCUSSION

We have shown that a truncated form of *E. coli* RNase III lacking the dsRBD can accurately cleave small RNase III substrates in vitro. The intrinsic catalytic activity of RNase III[ΔdsRBD] therefore validates use of the terms "catalytic domain" or "nuclease domain" to this portion of the RNase III polypeptide, which was hitherto based mainly on the effects of specific mutations on substrate cleavage. RNase III[ΔdsRBD] is sensitive to substrate reactivity epitopes, as it is inhibited by specific W−C bp antideterminant sequences in the proximal box or distal box which also inhibit RNase III. Assuming that the inhibitory W−C bp substitutions directly disrupt RNA−protein recognition, the data suggest that the catalytic domain may contact substrate up to one full helical turn from the cleavage site. Ethylation interference and hydroxyl radical footprinting experiments support the

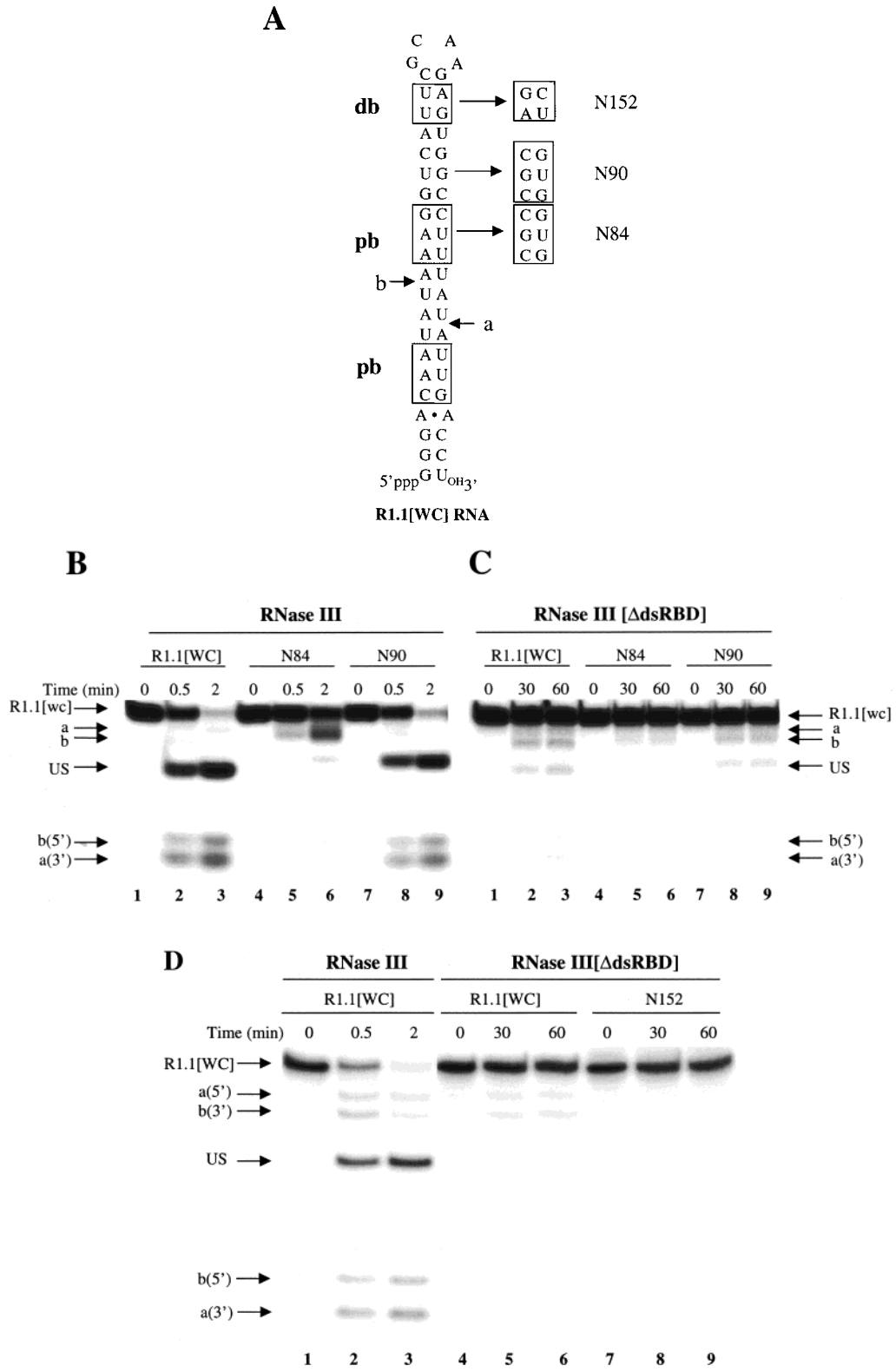

FIGURE 7: RNase III[ΔdsRBD] inhibition by substrate antideterminants. (A) Diagram of R1.1[WC] RNA. The boxed sequences represent the 3 bp proximal box (pb) and 2 bp distal box (db), in which specific W−C bp substitutions can inhibit cleavage (*8*). Shown to the right are the bp sequence substitutions present in the R1.1[WC] RNA variants N84, N90, and N152 RNA. The RNase III cleavage sites are indicated by "a" and "b". (B) RNase III cleavage of N84 RNA and N90 RNA. Reaction times are indicated, with the reaction buffer containing 300 mM NaCl, 5 mM Mg^{2+}, and 50 nM enzyme. (C) RNase III[ΔdsRBD] cleavage of N84 RNA and N90 RNA. The reaction times are indicated, with the reaction buffer containing 60 mM NaCl, 25 mM Mg^{2+}, and 100 nM enzyme. (D) RNase III and RNase III[ΔdsRBD] cleavage of N152 RNA. Reaction times are indicated. The reaction buffer for the experiment shown in lanes 1−3 was 300 mM NaCl, 5 mM Mg^{2+}, and 50 nM RNase III. For lanes 4−9 the reaction buffer included 60 mM NaCl, 25 mM Mg^{2+}, and 100 nM RNase III[ΔdsRBD].

existence of RNase III contacts distal to the cleavage site (*23*). That the dsRBD is not strictly required for cleavage site selection is consistent with the growing body of evidence that the motif does not exhibit bp sequence-specific binding

Table 2: Comparison of Effects of Antideterminant bp in the R1.1[WC] RNA Proximal Box or Distal Box on the Initial Rate of Cleavage by RNase III[ΔdsRBD] and RNase III[a]

substrate	RNase III	RNase III[ΔdsRBD]
R1.1[WC] RNA	(1.0)	(1.0)
N84 RNA	0.15	0.45
N152 RNA	0.17	0.32
N90 RNA	1.0	1.0

[a] The sequences of the N84, N152, and N90 RNA are provided in Figure 7A. The numbers represent the initial rate of cleavage of internally ^{32}P-labeled substrate by each enzyme, relative to the initial rate of cleavage of R1.1[WC] (normalized to 1.0). The reported numbers are the average of two experiments, with a maximum error of <30% for RNase III and <25% for RNase III[ΔdsRBD]. Experimental conditions are the same as those described in the legends to Figure 7B,D (RNase III) and Figure 7C,D (RNase III[ΔdsRBD].

(*18*, *19*). Instead, site-specificity in dsRNA cleavage is conferred by the N-terminal domain of the RNase III polypeptide. Other dsRNA-binding proteins may employ multiple dsRBDs with differing intrinsic binding affinities and specific relative positions, which can recognize RNA elements with complementary structural shapes (*18*, *19*). The dsRBD is not essential for RNase III dimer formation or stability, since it is shown elsewhere that RNase III[ΔdsRBD] retains dimeric behavior (A. K. Amarasinghe, S. Su, W.S., R. W. Simons, and A.W.N., in preparation). We have not yet been able to reconstitute RNase III processing activity in vitro by combining purified catalytic domain and dsRBD. The requirements for functional reconstitution are unclear but could involve the covalent linkage of the two domains.

RNase III[ΔdsRBD] retains strict specificity for dsRNA. In the first analysis this is not altogether surprising, since the domain formally must engage dsRNA prior to cleavage. However, the conserved specificity argues against a mechanism in which the dsRBD may alter (e.g., melt) dsRNA, such that the catalytic domain (perhaps one in each subunit) engages ssRNA prior to cleavage. The dsRNA specificity also implies that the catalytic domain contains a dsRNA-binding motif distinct from the dsRBD. Since the catalytic domain performs a chemical reaction, a significant change in dsRNA structure may be required to reach the transition state, which may be a unique capacity of this type of dsRNA-binding domain. This capability may not be accessible to the dsRBD, which has not been shown to possess catalytic activity or induce a significant change in dsRNA structure (*19*, *36*, *37*). A primary function of the dsRBD would be to provide binding affinity for cellular substrates which exhibit, among other features, a minimum double-helical length. This function of the dsRBD could also regulate an otherwise potentially toxic action of the catalytic domain. It is possible that the dsRBD may regulate substrate cleavage in a manner similar to dsRBD regulation of the dsRNA-dependent protein kinase PKR, which undergoes autophosphorylation and activation only upon dsRBD binding to dsRNAs possessing a specific minimum length (*38*).

The ability of ethidium bromide (EB) to inhibit RNase III[ΔdsRBD] is consistent with the ability of EB to block RNase III cleavage of substrate without affecting dsRBD-mediated binding (*29*). EB binding to substrate may prohibit binding of the catalytic domain or block a subsequent step such as phosphodiester hydrolysis. However, we have not been able to distinguish between the two possibilities, since the RNase III[ΔdsRBD]−substrate complex is too weak to be detected by gel shift or filter binding assays (unpublished observations). Regardless of the current technical limitations, the inhibitory action of EB is consistent with the specificity of the RNase III catalytic domain for dsRNA.

The combination of Mn^{2+} and low salt confers a catalytic efficiency comparable to that of RNase III in physiological salt and Mg^{2+}. These conditions may serve to enhance substrate binding, since low salt concentrations reduce ionic competition and Mn^{2+} promotes a higher affinity for substrate phosphodiesters (*39*). Alternatively (or in addition) low salt may promote divalent metal ion binding to enzyme, thereby enhancing activity. The difference in K_m values supports the argument for substrate affinity enhancement; however, this needs to be shown directly. Elevated concentrations of Mn^{2+} strongly inhibit RNase III[ΔdsRBD], similar to RNase III. We have shown elsewhere that inhibition is due to occupancy of an inhibitor (I) site, which this study has now firmly established to be localized to the catalytic domain and which is in part mediated by a specific carboxylic acid side chain (Glu 117) (*24*).

Secondary cleavage sites occur in RNAs which are not normally cleaved by RNase III and are positioned within short double-stranded regions, punctuated by bulges, loops, or base mismatches (*14*). On the basis of this study we believe that RNase III cleavage of secondary sites primarily reflects the action of the catalytic domain independent of the dsRBD. The combination of low salt and Mn^{2+} would provide the necessary affinity for otherwise unreactive substrates, thereby effectively bypassing the requirement of dsRBD engagement of a suitably sized double-helical segment. Previous studies suggested that RNase III may act as a Mn^{2+} metalloenzyme in vivo (*40*−*42*). However, there is no compelling evidence to support this proposal, since the intracellular Mn^{2+} concentration is low and since Mn^{2+}-dependent cleavage sites in vitro are not observed in vivo (e.g., see refs *14* and *43*).

The size of the RNase III[ΔdsRBD] polypeptide (∼18 kDa) is similar to that of *E. coli* RNase H1 (17.5 kDa) (*44*). We have proposed a similar catalytic mechanism for RNase III and RNase H1, on the basis of Mn^{2+} ion inhibition and the effect of mutation of a highly conserved glutamic acid (*24*). The similarity in size is not incompatible with such a proposal, even though there is little primary sequence similarity between the two enzymes. The conserved processing activity and double-strand-specificity of RNase III-[ΔdsRBD] suggests an evolutionary origin of RNase III involving fusion of an archetypal ∼17 kDa dsRNase to a dsRBD, thereby conferring additional specificity and regulation. The retained dimeric behavior of RNase III[ΔdsRBD] also suggests an early origin and conserved nature of this feature of RNase III structure.

Several higher eukaryotic RNase III orthologues have apparent tandem duplicated catalytic domains, as evidenced by two copies of the "signature sequence" and other conserved residues (*21*, *22*, *27*, *45*) (see Figure 1). Since the *E. coli* RNase III[ΔdsRBD] retains dimeric behavior as well as catalytic activity, the higher eukaryotic RNase III orthologues, if indeed dimeric in structure, would contain four active sites/dimer. A functional implication of a four-active-site holoenzyme is that cleavage of dsRNA could provide products of precisely defined lengths. Specifically, the

subunit structure (and therefore also the dimer structure) would necessarily impose a precise distance between active site pairs, thereby establishing a specific distance between coordinate cleavage sites. This would be consistent with the observation that the RNase III orthologue "*Dicer*", involved in the RNAi pathway, cleaves dsRNA to create short duplex products, ~22 bp in length (*28*, *46*, *47*). In contrast, *E. coli* RNase III cleaves dsRNA to provide a broader size range of products, 11−15 bp in length (*6*, *34*). Further studies on the structure and function of *E. coli* RNase III will shed new light on a conserved mechanism of dsRNA cleavage.

ACKNOWLEDGMENT

The authors thank Mike Hagen and Tara Twomey for DNA sequence analyses and Bob Simons for his insight and collaboration on structure−function studies of RNase III. The authors also thank other members of the Nicholson lab for their support and encouragement.

REFERENCES

1. Grunberg-Manago, M. (1999) *Annu. Rev. Genet. 33*, 193−227.
2. Nicholson, A. W. (1999) *FEMS Microbiol. Rev. 23*, 371−390.
3. Steege, D. A. (2000) *RNA 6*, 1079−1090.
4. Deutscher, M. P. (2000) *Prog. Nucleic Acid Res. Mol. Biol. 66*, 67−105.
5. Robertson, H. D., Webster, R. E., and Zinder, N. D. (1968) *J. Biol. Chem. 243*, 82−91.
6. Court, D. (1993) in *Control of Messenger RNA Stability* (Belasco, J. G., Brawerman, G., Eds). pp 71−116, Academic Press, NY.
7. Nicholson, A. W. (1996) *Prog. Nucleic Acids Res. Mol. Biol. 52*, 1−65.
8. Zhang, K., and Nicholson, A. W. (1997) *Proc. Natl. Acad. Sci. U.S.A. 94*, 13437−13441.
9. Chelladurai, B. S., Li, H., and Nicholson, A. W. (1991) *Nucleic Acids Res. 19*, 1759−1766.
10. Chelladurai, B. S., Li, H., Zhang, K., and Nicholson, A. W. (1993) *Biochem. 32*, 7549−7558.
11. Li, H., Chelladurai, B. S., Zhang, K., and Nicholson, A. W. (1993) *Nucleic Acids Res. 21*, 1919−1925.
12. Conrad, C., Rauhut, R., and Klug, G. (1998) *Nucleic Acids Res. 26*, 4446−4453.
13. Dunn, J. J. (1976) *J. Biol. Chem. 251*, 3807−3814.
14. Gross, G., and Dunn, J. J. (1987) *Nucleic Acids Res. 15*, 431−442.
15. Saito, H., and Richardson, C. C. (1981) *Cell 27*, 533−542.
16. Nashimoto, H., and Uchida, H. (1985). *Mol. Gen. Genet. 201*, 25−29.
17. Kharratt, A., Macia, M. J., Gibson, T. J., Nilges, M., and Pastore, A. (1995) *EMBO J. 14*, 3572−3584.
18. St. Johnston, D., Brown, N. H., Gall, J. G., and Jantsch, M. (1992) *Proc. Natl. Acad. Sci. U.S.A. 89*, 10979−10983.
19. Fiero-Monti, I., and Mathews, M. B. (2000) *Trends Biochem. Sci. 25*, 241−246.
20. Rotondo, G., and Frendewey, D. (1996) *Nucleic Acids Res. 24*, 2377−2386.
21. Mian, I. S. (1997) *Nucleic Acids Res. 25*, 3187−3195.
22. Aravind, L., and Koonin, E. V. (2001) *Methods Enzymol. 341*, 3−28.
23. Li, H., and Nicholson, A. W. (1996) *EMBO J. 15*, 101−113.
24. Sun, W., and Nicholson, A. W. (2001) *Biochemistry 40*, 5102−5110.
25. Dasgupta, S., Fernandez, L, Kameyama, L, Inada, T, Nakamura, Y, Pappas, A., and Court, D. L. (1998) *Mol. Microbiol. 28*, 629−640.
26. Lamontagne, B., Trembly, A., and Abou Elela, S. (2000) *Mol. Cell. Biol. 20*, 1104−1115
27. Jacobsen, S., Running, M. P., and Meyerowitz, E. M. (1999) *Development 126*, 5231−5243.
28. Bernstein, E., Caudy, A. A., Hammond, S. M., and Hannon, G. J. (2001) *Nature 409*, 363−366.
29. Calin-Jageman, I., Amarasinghe, A. K., and Nicholson, A. W. (2001) *Nucleic Acids Res. 29*, 1915−1925.
30. Amarasinghe, A. K., Calin-Jageman, I., Harmouch, A., Sun, W., and Nicholson, A. W. (2001). *Methods Enzymol. 342*, 143−158.
31. He, B., Rong, M., Lyakhov, D., Gartenstein, H., Diaz, G., Castagna, R., McAllister, W. T., and Durbin, R. K. (1997) *Protein Expression Purif. 9*, 142−151.
32. Dunn, J. J., and Studier, F. W. (1983) *J. Mol. Biol. 166*, 477−535.
33. Kindler, P., Keil, T. U., and Hofschneider, P. H. (1973) *Mol. Gen. Genet. 201*, 25−29.
34. Dunn, J. J. (1982) in *The Enzymes* (Boyer, P., Ed.) pp 485−499, Academic Press, New York.
35. Rudinger, J., Hillenbrandt, R., Sprinzl, M., and Giege, R. (1996) *EMBO J. 15*, 650−657.
36. Ryter, J. M., and Schultz, S. C. (1998) *EMBO J. 17*, 7505−7513.
37. Ramos, A, Bayer, P., and Varani G. (1999) *Biopolymers* 52, 181−196
38. Clemens, M. J. (1997) *Int. J. Biochem. Cell Biol. 29*, 945−949.
39. Cowan, J. A. (1998) *Chem. Rev. 98*, 1067−1088.
40. Srivastava, R. K., Miczak, A., and Apirion, D. (1990). *Biochimie 72*, 791−802.
41. Srivastava, R. A. K., Srivastava, N., and Apirion, D. (1992). *Int. J. Biochem. 24*, 737−749.
42. Makarov, E. M., and Apirion, D. (1992). *Biochem. Int. 26*, 1115−1124.
43. Paddock, G. V., Fukada, K., Abelson, J., and Robertson, H. D. (1976). *Nucleic Acids Res. 3*, 1351−1371.
44. Kanaya, S., and Crouch, R. J. (1983) *J. Biol. Chem. 258*, 1276−1281.
45. Matsuda, S., Ichigotani, Y., Okuda, T., Irimura, T., Nakatsugawa, S., and Hamguchi, M. (2000) *Biochim. Biophys. Acta 1490*, 163−169.
46. Hammond, S. M., Bernstein, E., Beach, D., and Hannon, G. J. (2000) *Nature 404*, 293−296.
47. Zamore, P. D., Tuschl, T., Sharp, P. A., and Bartel, D. P. (2000) *Cell 13*, 25−33.

BI011570U